Search for the neutral Higgs boson

L3 Collaboration

B. Adeva [a], O. Adriani [b], M. Aguilar-Benitez [c], H. Akbari [d], J. Alcaraz [c], A. Aloisio [e], G. Alverson [f], M.G. Alviggi [e], Q. An [g], H. Anderhub [h], A.L. Anderson [i], V.P. Andreev [j], T. Angelov [i], L. Antonov [k], D. Antreasyan [ℓ], P. Arce [c], A. Arefiev [m], T. Azemoon [n], T. Aziz [o], P.V.K.S. Baba [g], P. Bagnaia [p], J.A. Bakken [q], L. Baksay [r], R.C. Ball [n], S. Banerjee [o,g], J. Bao [d], L. Barone [p], A. Bay [s], U. Becker [i], J. Behrens [h], S. Beingessner [t], Gy.L. Bencze [u], J. Berdugo [c], P. Berges [i], B. Bertucci [p], B.L. Betev [k], A. Biland [h], R. Bizzarri [p], J.J. Blaising [t], P. Blömeke [v], B. Blumenfeld [d], G.J. Bobbink [w], M. Bocciolini [b], W. Böhlen [x], A. Böhm [v], T. Böhringer [y], B. Borgia [p], D. Bourilkov [k], M. Bourquin [s], D. Boutigny [t], B. Bouwens [w], J.G. Branson [z], I.C. Brock [aa], F. Bruyant [a], C. Buisson [ab], A. Bujak [ac], J.D. Burger [i], J.P. Burq [ab], J. Busenitz [ad], X.D. Cai [g], C. Camps [v], M. Capell [ac], F. Carbonara [e], F. Carminati [b], A.M. Cartacci [b], M. Cerrada [c], F. Cesaroni [p], Y.H. Chang [i], U.K. Chaturvedi [g], M. Chemarin [ab], A. Chen [af], C. Chen [ag], G.M. Chen [ag], H.F. Chen [ah], H.S. Chen [ag], M. Chen [i], M.C. Chen [ai], M.L. Chen [n], G. Chiefari [e], C.Y. Chien [d], F. Chollet [t], C. Civinini [b], I. Clare [i], R. Clare [i], H.O. Cohn [aj], G. Coignet [t], N. Colino [a], V. Commichau [v], G. Conforto [b], A. Contin [a], F. Crijns [w], X.Y. Cui [g], T.S. Dai [i], R. D'Alessandro [b], R. de Asmundis [e], A. Degré [a,t], K. Deiters [a,ak], E. Dénes [u], P. Denes [q], F. DeNotaristefani [p], M. Dhina [h], D. DiBitonto [ad], M. Diemoz [p], F. Diez-Hedo [a], H.R. Dimitrov [k], C. Dionisi [p], F. Dittus [ai], R. Dolin [i], E. Drago [e], T. Driever [w], D. Duchesneau [s], P. Duinker [w,a], I. Duran [a,c], H. El Mamouni [ab], A. Engler [aa], F.J. Eppling [i], F.C. Erné [w], P. Extermann [s], R. Fabbretti [h], G. Faber [i], M. Fabre [h], S. Falciano [p], Q. Fan [g,ag], S.J. Fan [aℓ], O. Fackler [ac], J. Fay [ab], J. Fehlmann [h], H. Fenker [f], T. Ferguson [aa], G. Fernandez [c], F. Ferroni [p,a], H. Fesefeldt [v], J. Field [s], F. Filthaut [w], G. Finocchiaro [p], P.H. Fisher [d], G. Forconi [s], T. Foreman [w], K. Freudenreich [h], W. Friebel [ak], M. Fukushima [i], M. Gailloud [y], Yu. Galaktionov [m], E. Gallo [b], S.N. Ganguli [o], P. Garcia-Abia [c], S.S. Gau [af], S. Gentile [p], M. Glaubman [f], S. Goldfarb [n], Z.F. Gong [g,ah], E. Gonzalez [c], A. Gordeev [m], P. Göttlicher [v], D. Goujon [s], G. Gratta [ai], C. Grinnell [i], M. Gruenewald [ai], M. Guanziroli [g], A. Gurtu [o], H.R. Gustafson [n], L.J. Gutay [ac], H. Haan [v], S. Hancke [v], K. Hangarter [v], M. Harris [a], A. Hasan [g], D. Hauschildt [w], C.F. He [aℓ], T. Hebbeker [v], M. Hebert [z], G. Herten [i], U. Herten [v], A. Hervé [a], K. Hilgers [v], H. Hofer [h], H. Hoorani [g], L.S. Hsu [af], G. Hu [g], G.Q. Hu [aℓ], B. Ille [ab], M.M. Ilyas [g], V. Innocente [e,a], E. Isiksal [h], E. Jagel [g], B.N. Jin [ag], L.W. Jones [n], R.A. Khan [g], Yu. Kamyshkov [m], Y. Karyotakis [t,a], M. Kaur [g], S. Khokhar [g], V. Khoze [j], M.N. Kienzle-Focacci [s], W. Kinnison [am], D. Kirkby [ai], W. Kittel [w], A. Klimentov [m], A.C. König [w], O. Kornadt [v], V. Koutsenko [m], R.W. Kraemer [aa], T. Kramer [i], V.R. Krastev [k], W. Krenz [v], J. Krizmanic [d], A. Kuhn [x], K.S. Kumar [an], V. Kumar [g], A. Kunin [m], A.van Laak [v], V. Lalieu [s], G. Landi [b], K. Lanius [a], D. Lanske [v], S. Lanzano [e], P. Lebrun [ab], P. Lecomte [h], P. Lecoq [a], P.Le Coultre [h], D. Lee [am], I. Leedom [f], J.M. Le Goff [a], L. Leistam [a], R. Leiste [ak], M. Lenti [b], J. Lettry [h], P.M. Levchenko [j], X. Leytens [w], C. Li [ah], H.T. Li [ag], J.F. Li [g], L. Li [h], P.J. Li [aℓ], Q. Li [g], X.G. Li [ag], J.Y. Liao [aℓ], Z.Y. Lin [ah], F.L. Linde [aa], D. Linnhofer [a], R. Liu [g], Y. Liu [g], W. Lohmann [ak], S. Lökös [r], E. Longo [p], Y.S. Lu [ag], J.M. Lubbers [w], K. Lübelsmeyer [v], C. Luci [a], D. Luckey [ℓ,i], L. Ludovici [p], X. Lue [h], L. Luminari [p], W.G. Ma [ah], M. MacDermott [h], R. Magahiz [r], M. Maire [t], P.K. Malhotra [o], R. Malik [g], A. Malinin [m], C. Maña [c], D.N. Mao [n],

 0370-2693/91/$ 03.50 © 1991 – Elsevier Science Publishers B.V. (North-Holland)

Y.F. Mao [ag], M. Maolinbay [h], P. Marchesini [g], A. Marchionni [b], J.P. Martin [ab], L. Martinez [a], F. Marzano [p], G.G.G. Massaro [w], T. Matsuda [i], K. Mazumdar [o], P. McBride [an], T. McMahon [ac], D. McNally [h], Th. Meinholz [v], M. Merk [w], L. Merola [c], M. Meschini [b], W.J. Metzger [w], Y. Mi [g], M. Micke [v], U. Micke [v], G.B. Mills [am], Y. Mir [g], G. Mirabelli [p], J. Mnich [v], M. Möller [v], B. Monteleoni [b], G. Morand [s], R. Morand [t], S. Morganti [p], R. Mount [ai], E. Nagy [u], M. Napolitano [c], H. Newman [ai], M.A. Niaz [g], L. Niessen [v], D. Pandoulas [v], F. Plasil [aj], G. Passaleva [b], G. Paternoster [e], S. Patricelli [e], Y.J. Pei [v], D. Perret-Gallix [t], J. Perrier [s], A. Pevsner [d], M. Pieri [b], P.A. Piroué [q], V. Plyaskin [m], M. Pohl [h], V. Pojidaev [m], N. Produit [s], J.M. Qian [i,g], K.N. Qureshi [g], R. Raghavan [o], G. Rahal-Callot [h], P. Razis [ad], K. Read [q], D. Ren [h], Z. Ren [g], S. Reucroft [f], S. Riemann [ak], O. Rind [n], C. Rippich [aa], H.A. Rizvi [g], B.P. Roe [n], M. Röhner [v], S. Röhner [v], U. Roeser [ak], Th. Rombach [v], L. Romero [c], J. Rose [v], S. Rosier-Lees [t], R. Rosmalen [w], Ph. Rosselet [y], J.A. Rubio [a,c], W. Ruckstuhl [s], H. Rykaczewski [h], M. Sachwitz [ak], J. Salicio [a,c], J.M. Salicio [c], G. Sanders [am], G. Sartorelli [ℓ,g], G. Sauvage [t], A. Savin [m], V. Schegelsky [j], D. Schmitz [v], P. Schmitz [v], M. Schneegans [t], M. Schöntag [v], H. Schopper [ao], D.J. Schotanus [w], H.J. Schreiber [ak], R. Schulte [v], S. Schulte [v], K. Schultze [v], J. Schütte [an], J. Schwenke [v], G. Schwering [v], C. Sciacca [e], I. Scott [an], R. Sehgal [g], P.G. Seiler [h], J.C. Sens [w], I. Sheer [z], V. Shevchenko [m], S. Shevchenko [m], X.R. Shi [aa], K. Shmakov [m], V. Shoutko [m], E. Shumilov [m], N. Smirnov [j], A. Sopczak [ai,z], C. Spartiotis [d], T. Spickermann [v], B. Spiess [x], P. Spillantini [b], R. Starosta [v], M. Steuer [ℓ,i], D.P. Stickland [q], W. Stoeffl [ae], B. Stöhr [h], H. Stone [s], K. Strauch [an], B.C. Stringfellow [ac], K. Sudhakar [o,v], G. Sultanov [g], R.L. Sumner [q], L.Z. Sun [ah], H. Suter [h], R.B. Sutton [aa], J.D. Swain [g], A.A. Syed [g], X.W. Tang [ag], E. Tarkovsky [m], L. Taylor [f], E. Thomas [g], C. Timmermans [w], Samuel C.C. Ting [i], S.M. Ting [i], Y.P. Tong [af], F. Tonisch [ak], M. Tonutti [v], S.C. Tonwar [o], J. Tòth [u], G. Trowitzsch [ak], K.L. Tung [ag], J. Ulbricht [x], L. Urbàn [u], U. Uwer [v], E. Valente [p], R.T. Van de Walle [w], H. van der Graaf [w], I. Vetlitsky [m], G. Viertel [h], P. Vikas [g], U. Vikas [g], M. Vivargent [t,i], H. Vogel [aa], H. Vogt [ak], M. Vollmar [v], G. Von Dardel [a], I. Vorobiev [m], A.A. Vorobyov [j], An.A. Vorobyov [j], L. Vuilleumier [y], M. Wadhwa [g], W. Wallraff [v], C.R. Wang [ah], G.H. Wang [aa], J.H. Wang [ag], Q.F. Wang [an], X.L. Wang [ah], Y.F. Wang [b], Z. Wang [g], Z.M. Wang [g,ah], J. Weber [h], R. Weill [y], T.J. Wenaus [i], J. Wenninger [s], M. White [i], R. Wilhelm [w], C. Willmott [c], F. Wittgenstein [a], D. Wright [q], R.J. Wu [ag], S.L. Wu [g], S.X. Wu [g], Y.G. Wu [ag], B. Wysłouch [i], Y.D. Xu [ag], Z.Z. Xu [ah], Z.L. Xue [aℓ], D.S. Yan [aℓ], B.Z. Yang [ah], C.G. Yang [ag], G. Yang [g], K.S. Yang [ag], Q.Y. Yang [ag], Z.Q. Yang [aℓ], C.H. Ye [g], J.B. Ye [h], Q. Ye [g], S.C. Yeh [af], Z.W. Yin [aℓ], J.M. You [g], M. Yzerman [w], C. Zaccardelli [ai], L. Zehnder [h], M. Zeng [g], Y. Zeng [v], D. Zhang [z], D.H. Zhang [w], Z.P. Zhang [ah], J.F. Zhou [v], R.Y. Zhu [ai], H.L. Zhuang [ag] and A. Zichichi [a,g]

[a] *European Laboratory for Particle Physics, CERN, CH-1211 Geneva 23, Switzerland*
[b] *INFN – Sezione di Firenze and University of Firenze, I-50125 Florence, Italy*
[c] *Centro de Investigaciones Energeticas, Medioambientales y Tecnologicas, CIEMAT, E-28040 Madrid, Spain*
[d] *Johns Hopkins University, Baltimore, MD 21218, USA*
[e] *INFN – Sezione di Napoli and University of Naples, I-80125 Naples, Italy*
[f] *Northeastern University, Boston, MA 02115, USA*
[g] *World Laboratory, FBLJA Project, CH-1211 Geneva, Switzerland*
[h] *Eidgenössische Technische Hochschule, ETH Zürich, CH-8093 Zurich, Switzerland*
[i] *Massachusetts Institute of Technology, Cambridge, MA 02139, USA*
[j] *Leningrad Nuclear Physics Institute, SU-188 350 Gatchina, USSR*
[k] *Central Laboratory of Automation and Instrumentation, CLANP, Sofia, Bulgaria*
[ℓ] *INFN – Sezione di Bologna, I-40126 Bologna, Italy*
[m] *Institute of Theoretical and Experimental Physics, ITEP, SU-117 259 Moscow, USSR*
[n] *University of Michigan, Ann Arbor, MI 48109, USA*
[o] *Tata Institute of Fundamental Research, Bombay 400 005, India*
[p] *INFN – Sezione di Roma and University of Rome "La Sapienza", I-00185 Rome, Italy*

[q] Princeton University, Princeton, NJ 08544, USA
[r] Union College, Schenectady, NY 12308, USA
[s] University of Geneva, CH-1211 Geneva 4, Switzerland
[t] Laboratoire de Physique des Particules, LAPP, F-74519 Annecy-le-Vieux, France
[u] Central Research Institute for Physics of the Hungarian Academy of Sciences, H-1525 Budapest 114, Hungary
[v] I. Physikalisches Institut, RWTH, W-5100 Aachen, FRG[1]
and III. Physikalisches Institut, RWTH, W-5100 Aachen, FRG[1]
[w] National Institute for High Energy Physics, NIKHEF, NL-1009 DB Amsterdam, The Netherlands
and NIKHEF-H and University of Nijmegen, NL-6525 ED Nijmegen, The Netherlands
[x] Paul Scherrer Institut (PSI), Würenlingen, Switzerland
[y] University of Lausanne, CH-1015 Lausanne, Switzerland
[z] University of California, San Diego, CA 92182, USA
[aa] Carnegie Mellon University, Pittsburgh, PA 15213, USA
[ab] Institut de Physique Nucléaire de Lyon, IN2P3-CNRS/Université Claude Bernard, F-69622 Villeurbanne Cedex, France
[ac] Purdue University, West Lafayette, IN 47907, USA
[ad] University of Alabama, Tuscaloosa, AL 35486, USA
[ae] Lawrence Livermore National Laboratory, Livermore, CA 94550, USA
[af] High Energy Physics Group, Taiwan, Rep. China
[ag] Institute of High Energy Physics, IHEP, Beijing, P.R. China
[ah] Chinese University of Science and Technology, USTC, Hefei, Anhui 230 029, P.R. China
[ai] California Institute of Technology, Pasadena, CA 91125, USA
[aj] Oak Ridge National Laboratory, Oak Ridge, TN 37830, USA
[ak] High Energy Physics Institute, O-1615 Zeuthen-Berlin, FRG
[al] Shanghai Institute of Ceramics, SIC, Shanghai, P.R. China
[am] Los Alamos National Laboratory, Los Alamos, NM 87544, USA
[an] Harvard University, Cambridge, MA 02139, USA
[ao] University of Hamburg, W-2000 Hamburg, FRG

Received 18 December 1990

We have searched for the neutral Higgs boson produced in decays of the Z^0 through the process $e^+e^- \to Z^0 \to H^0 Z^{0*}$. The data sample analysed corresponds to 111 200 hadronic decays of the Z^0. Combining the results of this analysis with previous L3 results we exclude a minimal standard model Higgs boson in the mass range $0 < M_{H^0} < 41.8$ GeV at the 95% confidence level.

1. Introduction

In the minimal standard model of electro-weak interactions [1] the existence of the neutral boson H^0 is required in order to give mass to the $W^\pm$ and the Z^0 vector bosons [2]. In this framework all the couplings of the H^0 boson both to the vector bosons and to the fermions are predicted, but its mass is left unpredicted. If the H^0 mass were lower than the Z^0 mass the Higgs boson would be produced at LEP through the Bjorken bremsstrahlung process [3]:

$$e^+e^- \to Z^0 \to H^0 + Z^{0*} \to H^0 + f\bar{f}\,.$$

Up to now there is no direct evidence for its existence and mass limits were reported by all LEP experiments [4–8].

In this paper we describe our search for the H^0 within the mass range from 15 to 50 GeV. This search used the data collected at LEP with the L3 detector in 1990 at centre of mass energies between 88.2 and 94.3 GeV. The total integrated luminosity is 5.3 pb^{-1}, corresponding to 111 200 hadronic Z^0 decays.

2. The L3 detector

The L3 detector covers 99% of 4π. The detector consists of a central tracking chamber, a high resolution electromagnetic calorimeter composed of BGO crystals, a ring of scintillation counters, a uranium and brass hadron calorimeter with proportional wire

[1] Supported by the German Bundesministerium für Forschung und Technologie.

chamber readout, and an accurate muon chamber system. These detectors are installed in a 12 m diameter magnet which provides a uniform field of 0.5 T along the beam direction.

The central tracking chamber is a time expansion chamber which consists of two cylindrical layers of 12 and 24 sectors, with 62 wires measuring the R–ϕ coordinate. The single wire resolution is 58 μm averaged over the entire cell. The double-track resolution is 640 μm. The fine segmentation of the BGO detector and the hadron calorimeter allows us to measure the direction of jets with an angular resolution of 2.5°, and to measure the total energy of hadronic events from Z^0 decay with a resolution of 10.2%. The muon detector consists of three layers of precise drift chambers, which measure 56 points on the muon trajectory in the bending plane, and eight points in the non-bending direction.

For the present analysis, we use the data collected in the following ranges of polar angle:
- for the central tracking chamber, $27° < \theta < 153°$,
- for the hadron calorimeter, $5° < \theta < 175°$,
- for the muon chambers, $35.8° < \theta < 144.2°$,
- for the electromagnetic calorimeter, $42.4° < \theta < 137.6°$.

The luminosity is determined by measuring small angle Bhabha events in two forward calorimeters consisting of BGO crystals. The detector and its performance are described in detail elsewhere [9,10].

3. H^0 production and decay

The $e^+e^- \to Z^0 \to H^0 + Z^{0*}$ cross section is predicted by the standard model and depends on the Higgs mass [11]. Higher order electro-weak corrections have been taken into account using the Improved Born Approximation [12] and adding the contribution of a top quark triangle graph at the $Z^0Z^{0*}H^0$ vertex [13]. The effect of initial state photon radiation has been computed using an exponentiation technique [14].

Since the Higgs coupling to fermions is proportional to the fermion mass, the Higgs decays predominantly into a $b\bar{b}$ pair for masses above 15 GeV, although the branching ratios into $c\bar{c}$ and $\tau^+\tau^-$ are not negligible [15]. QCD corrections [16] decrease the partial widths into $q\bar{q}$, thus enhancing the branching ratio into $\tau^+\tau^-$ compared to the tree level. After this correction the branching ratio into $\tau^+\tau^-$ for a Higgs of 40 GeV is approximately 6%.

We have carried out the search in the following three channels:

$$e^+e^- \to H^0\nu\bar{\nu}\,,$$

$$e^+e^- \to H^0\mu^+\mu^-\,,$$

$$e^+e^- \to H^0e^+e^-\,.$$

In order to study the production and decay of the Higgs boson, and to determine the acceptance of the detector and the efficiency of the selection, a Monte Carlo simulation of different processes has been performed. Higgs events were generated in the above channels for six different H^0 masses in the range from 15 to 50 GeV. The event generator program includes initial state photon radiation and final state radiation of photons from leptons and gluons from quarks. Different background sources have also been simulated as described below. Hadronisation and decays have been simulated using the Lund model (JETSET 6.3) [17] with parton shower fragmentation. The response of the detector has been simulated using the L3 detector simulation program [18] which takes into account the effects of energy loss, multiple scattering, interactions and decays in the detector materials and in the beam pipe. The resolution and the efficiency of the detector are also included in the simulation.

4. $Z^0 \to H^0\nu\bar{\nu}$ event selection

In the process $H^0\nu\bar{\nu}$ a large fraction of the energy is carried by the neutrinos. Depending on the Higgs mass and the Lorentz boost of the Higgs, the decay products can either be close to each other, appearing as a single jet, or be well separated in space, forming two or more jets. Thus the signatures are one jet or two acollinear jets or three acoplanar jets, large missing energy and large momentum imbalance. Jets are reconstructed using a two step procedure [10]: first neighbouring calorimetric hits are combined into *clusters*, then *jets* are formed merging neighbouring *clusters* and muon tracks. Each charged track measured in the vertex chamber is assigned to the nearest jet. The visible mass, M_{vis}, of the event is computed from calorimetric clusters and muon tracks assuming they correspond to massless particles. In order to

study the background contamination in detail we have simulated different processes: 168 000 hadronic decays of the Z^0, a number of $e^+e^- \to e^+e^- q\bar{q}$ events with invariant mass of the $q\bar{q}$ system greater than 4 GeV corresponding to 16.7 pb^{-1} and 9900 $e^+e^- \to \tau^+\tau^-(\gamma)$ events. We refer to these processes as "qq", "$\gamma\gamma$" and "$\tau\tau$" respectively.

We have implemented the following set of preselection cuts which reject the bulk of the background events:

(1) There should be at least four charged tracks with transverse momentum greater than 0.3 GeV and a distance of closest approach to the beam axis less than 10 mm.

(2) The energy deposited in the luminosity monitor should be less than 20 GeV.

(3) There should be at least one jet with all the following properties:
- at least 7 GeV of energy,
- at least 20° away from the beam axis,
- at least one track in the central tracking detector within 35° of the jet axis.

(4) The longitudinal energy imbalance should be less than 60% of the total visible energy.

(5) The transverse energy imbalance should be greater than 15% of the total visible energy.

(6) The visible mass of the event should be less than 65 GeV.

(7) There should not be more than three jets with energies greater than 5 GeV.

(8) If the event contains at least two jets, the angle between the two most energetic jets should be less than 3 rad.

These cuts are effective in decreasing the background from cosmics [cut (1)], beam-gas and beam-wall interactions [cuts (1) and (2)], two photon interactions [cuts (1)–(5)] and hadronic [cuts (5)–(8)] and tau [cuts (1) and (8)] decays of Z^0. The efficiency of these cuts for a 40 GeV Higgs signal is 87%. The visible mass of all the 364 surviving events is shown in fig. 1a for the data together with the Monte Carlo predictions for the background. Fig. 1b shows the corresponding Monte Carlo distribution for a Higgs of 40 GeV mass. All Monte Carlo histograms in fig. 1 are normalized to the total integrated luminosity. We estimate that after these cuts the background from sources other than qq, $\tau\tau$ and $\gamma\gamma$ events is negligible.

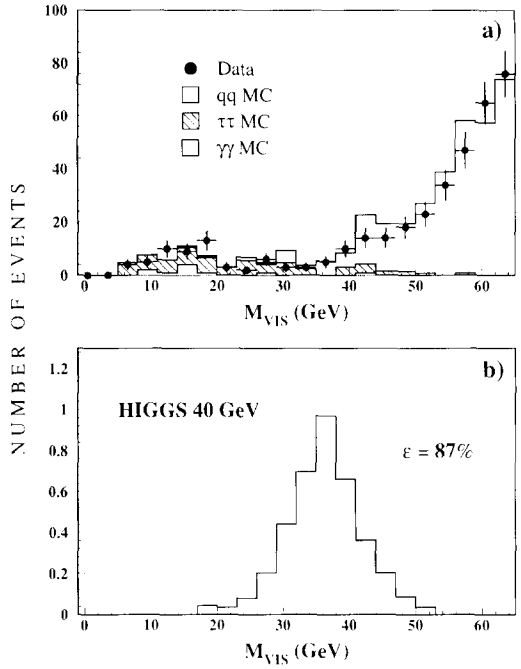

Fig. 1. (a) The invariant mass spectrum of data which pass the preselection for the $H^0\nu\bar{\nu}$ channel search (points) together with the Monte Carlo predictions (histogram) of the main sources of background: $q\bar{q}$, $e^+e^-q\bar{q}$ and $\tau^+\tau^-$ events; Monte Carlo events are normalized to the total integrated luminosity. (b) The invariant mass spectrum for 40 GeV Higgs Monte Carlo events.

In order to check how accurately the different background sources are reproduced by the Monte Carlo and to have an additional tool to separate the signal from the background we have used a χ^2 method [19]. We consider a class C of events, where C can be either qq or $\tau\tau$ or $\gamma\gamma$ or Higgs Monte Carlo events, and describe an event belonging to this class using the vector $\boldsymbol{x}$ with the following components:
- x_1: total visible energy;
- x^2: total imbalance;
- x_3: transverse energy imbalance;
- x_4: number of calorimetric clusters;
- x_5: angle between the two most energetic jets;
- x_6: angle between the plane of the two most energetic jets and the beam-axis.

The class C is then characterized by the covariance matrix

$$D_{ij} = \frac{1}{N} \sum_{k=1,\dots,N} (x_i^k - \bar{x}_i)(x_j^k - \bar{x}_j), \quad i,j = 1, \dots, 6 ,$$

where N is the total number of events in C. The dis-

tance of a given event, described by a vector y, from the class C is defined as

$$R_C = \frac{1}{N} \sum_{k=1,\dots,N} \sum_{i,j=1,\dots,6} (y_i - x_i^k) D_{ij}^{-1} (y_j - x_j^k) .$$

Finally we define the weight of the event, described by y, with respect to C,

$$W_C = \exp\left(-\tfrac{1}{12} R_C\right) ,$$

where the denominator in the exponent is twice the number of vector components.

We compute the weights W_{qq}, $W_{\tau\tau}$, $W_{\gamma\gamma}$ and W_H using the Monte Carlo samples of events satisfying the preselection criteria. The Higgs weight is interpolated, using the visible mass of the event, between the weights with respect to the two Higgs Monte Carlo samples with masses nearest to M_{vis}.

After defining these four weights we label each event as

qq-like if $W_{qq} > W_{\tau\tau}, W_{\gamma\gamma}$,

$\tau\tau$-like if $W_{\tau\tau} > W_{qq}, W_{\gamma\gamma}$,

$\gamma\gamma$-like if $W_{\gamma\gamma} > W_{qq}, W_{\tau\tau}$.

Fig. 2a shows the distributions of the difference $W_H - W_{qq}$ for the qq-like events from the data, the qq-like events from the Monte Carlo of the three main backgrounds and for all 40 GeV Higgs Monte Carlo event. We can see that the contribution from the $\tau\tau$ and $\gamma\gamma$ background is negligible. Fig. 2b shows the corresponding distributions for the $\tau\tau$-like events, where in this case the contribution from qq and $\gamma\gamma$ background is negligible.

To select the final sample we define the following variables:

(i) If the event contains at least three jets we consider the three most energetic jets and we define

$$\theta_{123} = \tfrac{1}{2}(\theta_{12} + \theta_{23} + \theta_{13}) ,$$

where θ_{ij} is the angle between jets i and j. In the case there are only two jets θ_{123} is the angle between the two jets and in the case there is only one jet θ_{123} is zero.

(ii) We find the minimum opening angle cone which contains all calorimetric energy, allowing at most 1 GeV outside the cone. We define

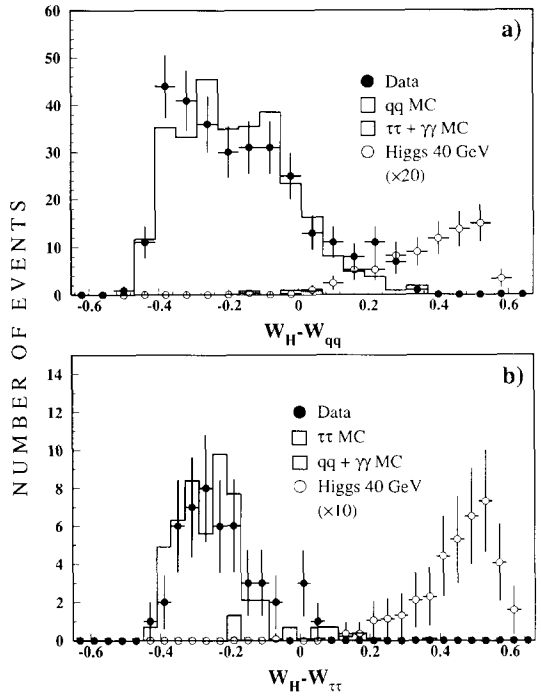

Fig. 2. The distributions for data and Monte Carlo of the quantities $W_H - W_{qq}$ (a) and $W_H - W_{\tau\tau}$ (b). The figures include only the events which have, respectively, a qq or $\tau\tau$ weight larger than the other two background weights. The distribution of these variables for a 40 GeV Higgs is also shown.

$$E^* = \frac{\sum_i E_i \cos\alpha_i}{\sum_i E_i} ,$$

where E_i is the energy either of a calorimetric cluster or of a muon track and α_i is the angle between its direction and the cone axis.

(iii) We define the background weight as

$$W_{BG} = \max(W_{qq}, W_{\tau\tau}, W_{\gamma\gamma}) .$$

An event is accepted if it satisfies the following criteria:

(a) $\theta_{123} < 3$ rad. The effect of this cut on the preselected sample is shown in fig. 3a. For $\theta_{123} > 3$ rad the number of events is already reduced by the preselection cut (8).

(b) $E^* > 0.12$. Fig. 3b shows E^* for all the events which survive cut (a).

(c) $W_H - W_{BG} > 0.14$. Fig. 3c shows this difference for all the events surviving cuts (a) and (b). The cut

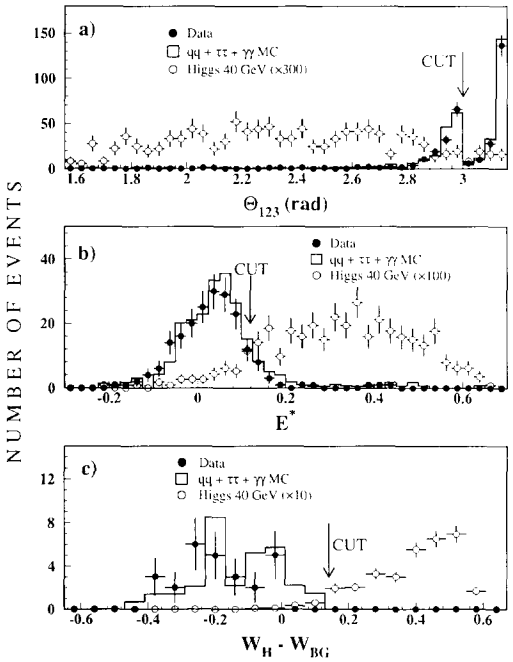

Fig. 3. The effect of the final three cuts for the $H^0\nu\bar{\nu}$ search applied sequentially to the preselected data. The arrows indicate the position of the cuts, (a) $\theta_{123}<3$ rad, (b) $E^*>0.12$, (c) $W_H - W_{BG}>0.14$.

Table 1
Detection efficiency for Higgs events in different channels.

Higgs mass [GeV]	$H^0\nu\nu$ [%]	$H^0\mu^+\mu^-$ [%]	$H^0e^+e^-$
15	42	54	40
20	57	60	41
30	70	62	39
40	68	61	38
45	61	61	38
50	47	59	35

is placed so as to reject all background Monte Carlo events.

The efficiency of these cuts versus the H^0 mass is shown in table 1. The trigger efficiency is included and it is found to be in excess of 99% in the mass range under investigation [4].

No events surviving these cuts were found in our data sample.

5. $Z^0 \to H^0e^+e^-$ and $Z^0 \to H^0\mu^+\mu^-$ event selection

$Z^0 \to H^0\ell^+\ell^-$ events are characterized by the presence of two high momentum isolated leptons, coming from the off-shell Z^{0*}, recoiling against one or more hadronic jets coming from the H^0 decay. In our case the two charged leptons can be either electrons or muons.

The identification of $H^0e^+e^-$ candidates is mainly based on energy deposition in the BGO barrel. For isolated electromagnetic clusters the quantity E_9/E_{25}, defined as the ratio of the energy deposited in a 3×3 crystal array and the energy deposited in a 5×5 array both centred on the same most energetic crystal, is approximately a gaussian centred at 1 with a width of 1%. A position-dependent leakage correction is applied to both energy measurements. An electron is identified as a cluster having E_9/E_{25} between 0.97 and 1.03 and a track in the central tracking chamber matching the cluster centroid with 5 mrad in the azimuthal angle.

Events are selected if two electrons are found, one with energy greater than 10 GeV, the other with energy greater than 7 GeV. Each electron must pass an isolation cut which requires that the additional energy in the BGO and hadron calorimeters within 10° of the electron direction is less than 5% of the electron energy.

If the sum of the energies of the two electrons exceeds 60% of $\sqrt{s}$ and the total number of calorimetric clusters is less than 10 an event is rejected. This cut removes radiative dilepton final states.

A further set of cuts is applied to the remaining sample in order to identify the Higgs signal. We require at least two tracks in the central chamber and one jet in the calorimeters, besides the ones associated with the electrons.

The detection efficiency for Higgs masses ranging from 15 to 50 GeV is shown in table 1.

One event out of the total data sample, identified as $e^+e^- \to e^+e^-\mu^+\mu^-$, passes the above selection criteria. The invariant mass of the $\mu^+\mu^-$ system was measured to be 0.4 GeV and is therefore outside the mass range under investigation. The event is consistent with the expected rate of four fermion final states.

The $H^0\mu^+\mu^-$ candidates are selected requiring that the event contains at least one track in the muon chambers with $P_\mu > 10$ GeV coming from the vertex

and associated with at least one hit in the scintillator barrel within 5 ns from the beam crossing.

For the detection of the Higgs decay products we require that at least five calorimetric clusters (of which two are associated with charged tracks) are present besides the ones associated with the muons. This cut removes cosmic rays and Z^0 decays into muon and tau pairs even if accompanied by photons, and four fermion final states.

In the case a second muon track with $P_\mu > 3$ GeV is present in the event we require that the invariant mass of the two muons should be larger than 5 GeV.

In the case only one muon track has been detected we require that
- the muon should be well inside the acceptance of the muon spectrometer: $|\cos\theta_\mu| < 0.75$;
- the thrust of the event should be less than 0.9.

Finally in order to remove hadronic (mainly $b\bar{b}$) decays of the Z^0 containing a muon in the final state at least one of the muons is required to be isolated. A muon is defined to be isolated if, within a cone of half angle 35° around it, there are less than two tracks in the vertex chamber, and a calorimetric energy less than 25% of the muon momentum, excluding tracks and energy associated with the muon.

The detection efficiency for a Higgs of 40 GeV mass is about 60%. The efficiency for different Higgs masses is shown in table 1.

No events survive these cuts both in the data and in a Monte Carlo sample of standard Z^0 decays corresponding to about 1.5 times the acquired luminosity.

The trigger efficiency for both lepton channels has been checked using electron, muon and tau pair events and has been found to be close to 100% due to the redundancy of the muon, energy and charged track triggers used.

6. Systematic uncertainties

The source of systematic errors on the number of expected Higgs events are the following:

(1) Theoretical uncertainty on the Higgs boson production cross section of 2%.

(2) Theoretical uncertainty on the Higgs decay branching ratios which contributes an error on the detection efficiency of 1%.

(3) Error on the Higgs detection efficiency of 2% due to the uncertainties in the Monte Carlo fragmentation parameters which was estimated varying the relevant Lund fragmentation parameters.

(4) Error on the luminosity [20] of 1.3%.

(5) Error on Higgs detection efficiency due to Monte Carlo statistics of 1.5%.

Combining all these errors in quadrature we obtain an overall systematic uncertainty of 4%.

For the neutrino channel we also studied $q\bar{q}\gamma$ events with a hard γ in order to compare the quantities used in the analysis between data and Monte Carlo. When these events are reconstructed ignoring the photon their topology is similar to the $H^0\nu\bar{\nu}$ events [6]. Fig. 4 shows the results of this comparison as well as the resolution on the invariant mass of the hadronic system. Data and Monte Carlo agree within the statistical errors.

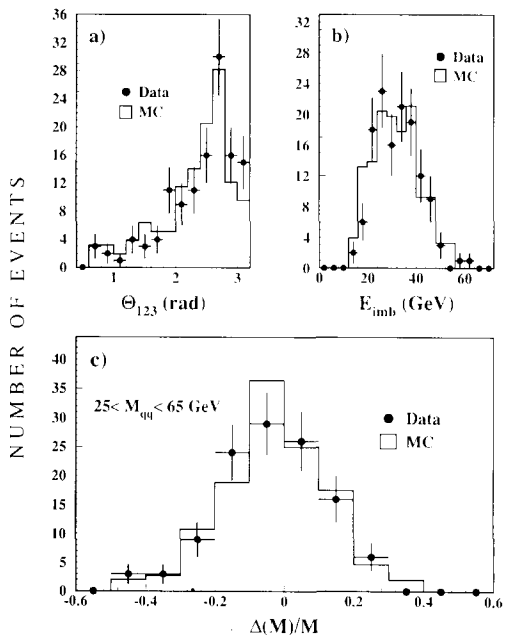

Fig. 4. Comparison of the data and the Monte Carlo for $q\bar{q}\gamma$ events, after removing the photon from the reconstruction. θ_{123} (a) and the total energy imbalance (b) are shown. The histogram represents the Monte Carlo and the points represent the data. In (c) the relative difference between the visible mass of the event, excluding the photon, and the invariant mass of the hadronic system computed from the energy of the photon is shown. The resolution for the visible mass is 15%.

7. Results and conclusions

Fig. 5 shows the expected number of events as a function of the Higgs mass for the different channels analysed. Since no events survive our cuts, combining the results from all three processes we exclude a minimal standard model Higgs boson in the mass range $15 < M_{H^0} < 41.8$ GeV at the 95% confidence level. The effect of the systematic error has been taken into account. Combining the result of this study with our previously published ones [4,5], we exclude a minimal standard model Higgs boson with a mass less than 41.8 GeV at the 95% confidence level. This result is in agreement with previous published measurements [6–8].

Acknowledgement

We wish to express our gratitude to the CERN accelerator divisions for the excellent performance of the LEP machine. We acknowledge the effort of all engineers and technicians who have participated in the construction and maintenance of this experiment.

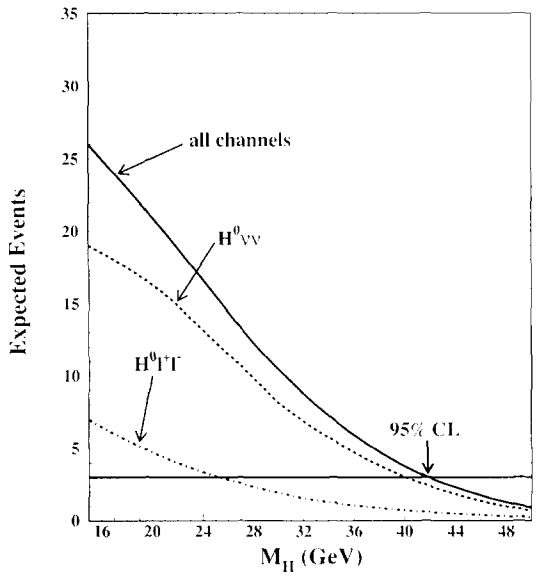

Fig. 5. The total number of events expected in the different channels. The mass limit corresponding to the 95% confidence level is indicated.

References

[1] S.L. Glashow, Nucl. Phys. 22 (1961) 579;
S. Weinberg, Phys. Rev. Lett. 19 (1967) 1264;
A. Salam, in: Elementary particle theory, ed. N. Svartholm (Almquist and Wiksell, Stockholm, 1968) p. 367.
[2] P.W. Higgs, Phys. Lett. 12 (1964) 132; Phys. Rev. Lett. 13 (1964) 508; Phys. Rev. 145 (1966) 1156;
F. Englert and R. Brout, Phys. Rev. Lett. 13 (1964) 321.
[3] J.D. Bjorken, in: Proc. 1976 SLAC Summer Institute on Particle physics (Stanford), ed. M.C. Zipf (Stanford Linear Accelerator Center, Stanford, CA, 1977) p. 1;
J. Finjord, Phys. Scr. 21 (1980) 143.
[4] L3 Collab., B. Adeva et al., Phys. Lett. B 248 (1990) 203.
[5] L3 Collab., B. Adeva et al., Phys. Lett. B 252 (1990) 518.
[6] ALEPH Collab., D. Decamp et al., Phys. Lett. B 246 (1990) 306.
[7] DELPHI Collab., P. Abreu et al., Nucl. Phys. B 342 (1990) 1; preprint CERN-PPE/90-163 (1990).
[8] OPAL Collab., M.Z. Akrawy et al., Phys. Lett. B 236 (1990) 224; 251 (1990) 211; B 253 (1991) 511.
[9] L3 Collab., B. Adeva et al., Nucl. Instrum. Methods A 289 (1990) 35.
[10] O. Adriani et al., preprint CERN-PPE/90-158 (1990), Nucl. Instrum. Methods, to be published.
[11] F.A. Berends and R. Kleiss, Nucl. Phys. B 260 (1985) 32.
[12] M. Consoli and W. Hollik, in: Z physics at LEP1, CERN report CERN-89-08, eds. G. Altarelli, R. Kleiss and C. Verzegnassi (CERN, Geneva, 1989) Vol. 1, p. 39.
[13] S. Dawson and S. Willebrock, Phys. Lett. B 211 (1988) 200;
Z. Hioki, Phys. Lett. B 224 (1989) 417.
[14] F.A. Berends, W.L. van Neerven and G.J.H. Burgers, Nucl. Phys. B 297 (1988) 429.
[15] P.J. Franzini et al., in: Z physics at LEP1, CERN report CERN-89-08, eds. G. Altarelli, R. Kleiss and C. Verzegnassi (CERN, Geneva, 1989) Vol. 2, p. 59, and references therein.
[16] E. Braaten and J.P. Leveille, Phys. Rev. D 22 (1980) 715.
[17] T. Sjöstrand and M. Bengtsson, Comput. Phys. Commun. 43 (1987) 367;
T. Sjöstrand, in: Z physics at LEP1, CERN report CERN-89-08, eds. G. Altarelli, R. Kleiss and C. Verzegnassi (CERN, Geneva, 1989) Vol. 3, p. 143.
[18] The L3 detector simulation is based on GEANT version 3.13 (September, 1989), see R. Brun et al., GEANT 3, CERN DD/EE/84-1 (revised) (September 1987);
the GHEISHA program is used to simulate hadronic interactions, H. Fesefeldt, RWTH Aachen preprint PITHA 85/02 (1985).
[19] See for example W. Hamilton, Statistics in physical science (New York, 1964).
[20] L3 Collab., B. Adeva et al., Phys. Lett. B 249 (1990) 341.